Journal of Environmental Management 319 (2022) 115747

Contents lists available at ScienceDirect

Journal of Environmental Management

journal homepage: www.elsevier.com/locate/jenvman

Research article

Modelling and techno-economic assessment of (bio)electrochemical nitrogen removal and recovery from reject water at full WWTP scale

Veera Koskue [a,*], Veli-Pekka Pyrhönen [a], Stefano Freguia [b], Pablo Ledezma [c], Marika Kokko [a]

[a] Faculty of Engineering and Natural Sciences, Tampere University, Korkeakoulunkatu 8, 33720 Tampere, Finland
[b] Department of Chemical Engineering, The University of Melbourne, Grattan Street, Parkville, VIC 3010, Australia
[c] Australian Centre for Water and Environmental Biotechnology, University of Queensland, Gehrmann Laboratories Building (60), Brisbane, QLD 4072, Australia

ARTICLE INFO

Keywords:
Bioelectrochemistry
BSM2
Centrate
Electrochemistry
Nutrient recovery
Wastewater treatment

ABSTRACT

At conventional wastewater treatment plants (WWTPs), reject waters originating from the dewatering of anaerobically digested sludge contain the highest nitrogen concentrations within the plant and thereby have potential for realising nitrogen recovery in a reusable form. At the same time, nitrogen removal from reject waters has potential to reduce the energetic and chemical demands of the WWTP due to a reduced nutrient load to the activated sludge process. In recent years, (bio)electrochemical methods have been extensively studied for nitrogen recovery from reject waters in laboratory-scale but not yet implemented in real WWTP environments, particularly due to concerns about the need for large capital investments. This study assessed the techno-economic feasibility of retrofitting a (bio)electrochemical nitrogen removal and recovery (NRR) unit into the reject water circulation line of a full-scale WWTP through modelling. Data from laboratory-scale (bio)electro-concentration ((B)EC) experiments was used to construct a simple, semi-empirical model block integrated into the Benchmark Simulation Model No. 2 (BSM2) simulating a generalised WWTP. The effects of nitrogen removal from the reject water on both the effluent quality and operational costs of the WWTP were assessed and compared to the BSM2 performance without an NRR unit. In all studied scenarios, the effluent quality index was improved by 4–11%, while both the aeration (7–19% decrease) and carbon (24–71%) requirements were reduced. The additional energy consumed by the NRR unit increased the total operational cost index by >18%, but the revenue assumed for the generated nutrient product (20 EUR kg_N^{-1}) was enough to make the BEC-NRR scenarios at realistically low current densities (1 and 5 A m^{-2}) economically attractive compared to the control. A sensitivity analysis revealed that electricity price and nutrient product value had the most notable effects on the feasibility of the NRR unit. The results suggest a key factor in making (bio)electrochemical NRR economically viable is to reduce its electricity consumption further, while the anticipated increases in nitrogen fertiliser prices can help accelerate the adoption of these methods in larger scale.

1. Introduction

Conventional wastewater treatment plants (WWTPs) are increasingly regarded as water resource recovery facilities (WRRFs), reflecting a shift in focus from solely looking at effluent water quality to also recognising the value of nutrients, energy, water and other resources contained in wastewaters (Flores-Alsina et al., 2021; Solon et al., 2019; Vaneeckhaute et al., 2018). One of the key resources that can be recovered from municipal wastewaters are nutrients, especially nitrogen, phosphorus and potassium. Phosphorus and potassium are both finite mineral resources that are mined for fertiliser use (Sutton et al., 2013), which is why more efficient reuse of these nutrients is vital in ensuring their sufficiency in the future.

Nitrogen, on the other hand, is a renewable gaseous resource, vastly present in our atmosphere (Erisman et al., 2008). While there is no scarcity of this element, nitrogen fertiliser production via transforming the unreactive atmospheric nitrogen to reactive nitrogen (such as ammonium nitrogen, NH_4–N) is very energy-intensive, contributing up to 2% of all energy usage in the world (Sutton et al., 2013). NH_4–N generation depends heavily on the use of fossil fuels, which leads to gaseous emissions and other environmental issues (Sutton et al., 2013; Wang et al., 2021) and makes nitrogen fertiliser prices very susceptible

* Corresponding author.
E-mail address: veera.koskue@tuni.fi (V. Koskue).

https://doi.org/10.1016/j.jenvman.2022.115747
Received 7 March 2022; Received in revised form 29 June 2022; Accepted 10 July 2022
Available online 15 July 2022

to shifts in the energy market rates. During 2021, for example, an increase in the rate of natural gas led to the doubling of nitrogen fertiliser prices (DTN, 2021; IFA, 2021). With the growing human population, the demand for nitrogen fertilisers and thereby their price are expected to increase even further in the future (Solon et al., 2019; Sutton et al., 2013). At the same time, the human interference with the nitrogen cycle has led to excess reactive nitrogen accumulating in the environment and thereby manifoldly exceeding the planetary boundary for reactive nitrogen, leading to severe pollution of, e.g., water bodies (Rockström et al., 2009). Recovering and recycling the already existing reactive nitrogen has become essential in mitigating this environmental deterioration, while also being a cost-effective alternative to the industrial processes considering the anticipated increases in nitrogen fertiliser production costs.

Due to the dilute nature of the influent wastewater, nutrient recovery strategies are often implemented to other, more nutrient-rich streams within the WWTPs. Anaerobic digestion (AD) is a commonly used strategy for sludge management at WWTPs, and the dewatering of the digested sludge results in the formation of the most nutrient-rich water stream within the plant, i.e., reject water (Fux and Siegrist, 2004; Wu and Modin, 2013). Reject waters from AD typically contain around 1 $g_{NH4\text{-}N}\,L^{-1}$ and contribute notably up to 25% of the total nitrogen load to the WWTP, as they are commonly recirculated back to the head of the treatment line to remove the nitrogen before discharge (Fux and Siegrist, 2004; Nancharaiah et al., 2016; Wu and Modin, 2013). This consequently increases the energy needs of the plant, as nitrogen is mainly removed from wastewater via the heavily-aerated activated sludge process (Metcalf and Eddy, 2014). Furthermore, wastewater is often deficient in organic matter, which is why an external carbon source addition is commonly required to get the carbon to nitrogen ratio at an optimal level for the biological nitrogen removal processes (Daigger, 2014). Both the requirement for aeration and external carbon addition directly depend on the nitrogen load to the activated sludge process, which is why nitrogen removal and recovery from reject waters has the potential to reduce both (Volcke et al., 2006).

To date, anaerobic ammonium oxidation (Anammox) has shown the greatest potential for energy-efficient reject water treatment to reduce the nitrogen load to the main wastewater treatment line and thereby lower the treatment costs (Fux and Siegrist, 2004; Lackner et al., 2014). However, the shortcoming of Anammox is that the NH_4–N is released as N_2 gas and cannot be recovered in a reusable form (Fux and Siegrist, 2004). Indeed, no technique capable of effectively recovering nitrogen has been widely established within municipal WWTPs yet (Solon et al., 2019). Nitrogen can be partly recovered from reject waters (<40%) through phosphate-based recovery processes, such as struvite precipitation (Vaneeckhaute et al., 2017). Ammonia stripping, which facilitates the selective recovery of nitrogen, is also a mature technology implemented at some full-scale WWTPs (Giordano et al., 2019; Vaneeckhaute et al., 2017) but its wider adaptation has been hindered by its high energy consumption. Furthermore, both struvite precipitation and ammonia stripping typically require chemical additions (Jaffer et al., 2002; Vaneeckhaute et al., 2017), which add to their operational costs (OPEX). As a result, more sustainable alternatives are continuously being developed. For example, (bio)electrochemical systems ((B)ESs) have been extensively studied for nitrogen recovery from reject waters in laboratory-scale (Desloover et al., 2012; Guo et al., 2020; Koskue et al., 2021a, 2021b; Rodrigues et al., 2020; Wu and Modin, 2013), showing great promise with recovery efficiencies up to 88% (Guo et al., 2020) at energy usages as low as 5 kWh kg_N^{-1} (Rodrigues et al., 2020). However, apart for some pilot-scale trials (Ward et al., 2018), (B)ESs for nutrient recovery are yet to be implemented in full scale.

Before implementing an emerging technology in full scale, modelling can be a useful tool to estimate the general feasibility of its incorporation into a WWTP. Plant-wide modelling is extremely complicated due to the complexity of the biological and biochemical processes involved. To address this problem, an International Water Association (IWA) task group developed and provided a freely available modelling tool depicting a generalised full-scale WWTP, the Benchmark Simulation Model No. 2 (BSM2) (Alex et al., 2018; Gernaey et al., 2014). The BSM2 includes the commonly used biological activated sludge process and sludge handling via AD, and therefore facilitates the evaluation of different nutrient removal/recovery options from the reject water stream and their effects on the overall plant performance (Flores-Alsina et al., 2021; Volcke et al., 2006).

So far, the nitrogen removal and/or recovery strategies for reject waters modelled in the BSM2 environment have focused on more established technologies, such as struvite precipitation and Anammox combined with partial nitritation or single reactor system for high activity ammonia removal over nitrite (SHARON) (Flores-Alsina et al., 2021; Volcke et al., 2006). At the same time, understanding the effects and economics of retrofitting emerging technologies, such as (bio)electrochemical nitrogen removal and recovery (NRR) systems, into the reject water recirculation of an existing WWTP will be a crucial step towards potential full-scale implementation and commercialisation in the future. Therefore, this study aimed at assessing the feasibility of implementing a (bio)electroconcentration cell ((B)EC) for NRR from reject water by developing a simple, semi-empirical NRR unit model based on laboratory-scale nitrogen recovery experiments (Koskue et al., 2021a, 2021b). The effect of the NRR unit on the BSM2 plant performance was then evaluated through dynamic simulations, using the BSM2 evaluation criteria. Based on the simulation data, a detailed economic analysis including the changes in the OPEX, the estimated capital investments (CAPEX) and a sensitivity analysis was carried out.

2. Materials and methods

2.1. Wastewater treatment plant model

The BSM2 (BSM2_R2019b MATLAB/Simulink implementation; Fig. 1) was used to model a conventional WWTP with AD for primary and secondary sludge treatment (Alex et al., 2018; Gernaey et al., 2014). The BSM2 utilises the Anaerobic Sludge Model No. 1 (ASM1) and the Anaerobic Digestion Model No.1 (ADM1) with appropriate interfaces (Alex et al., 2018; Gernaey et al., 2014). The influent wastewater was dynamically modelled using the BSM2 influent generator (Gernaey et al., 2006, 2011, 2014), assuming 80 000 person equivalents in the catchment area (Gernaey et al., 2011), which resulted in an average influent dry-weather flow rate of 20 648 $m^3\,d^{-1}$ (Alex et al., 2018; Gernaey et al., 2014). More details about the BSM2 model can be found in Appendix A in the Supplementary Material.

2.2. Nitrogen removal and recovery unit model

Results from laboratory-scale experiments with three-chamber (B)EC set-ups for nitrogen recovery from real reject water (Koskue et al., 2021a, 2021b) were used as a basis for developing a simple semi-empirical NRR unit model block (Fig. 2). In the (B)ECs, a concentrate chamber is created between an anode and a cathode chamber using cation- and anion-exchange membranes. The cationic NH_4–N permeates through the cation-exchange membrane and is recovered into the liquid concentrate (see Fig. S3 for more details on the operational principle).

The NRR unit was added to the reject water recirculation line within the BSM2 (Fig. 1), as reject water contains a large fraction of the NH_4–N circulating within the plant in a concentrated form (see Figs. S1–S2 and Table S1 for examples of the nitrogen loads in different parts of the WWTP). Two different versions of the NRR unit model were developed, utilising model parameters largely derived from the respective laboratory experiments: a biological NRR (BEC-NRR) (Koskue et al., 2021b), and a purely electrochemical NRR (EC-NRR) (Koskue et al., 2021a). Details about the dimensioning of the NRR unit model can be found in Appendix A and Table S2 of the Supplementary Material.

The NRR unit model block used the ASM1 state variables, namely the

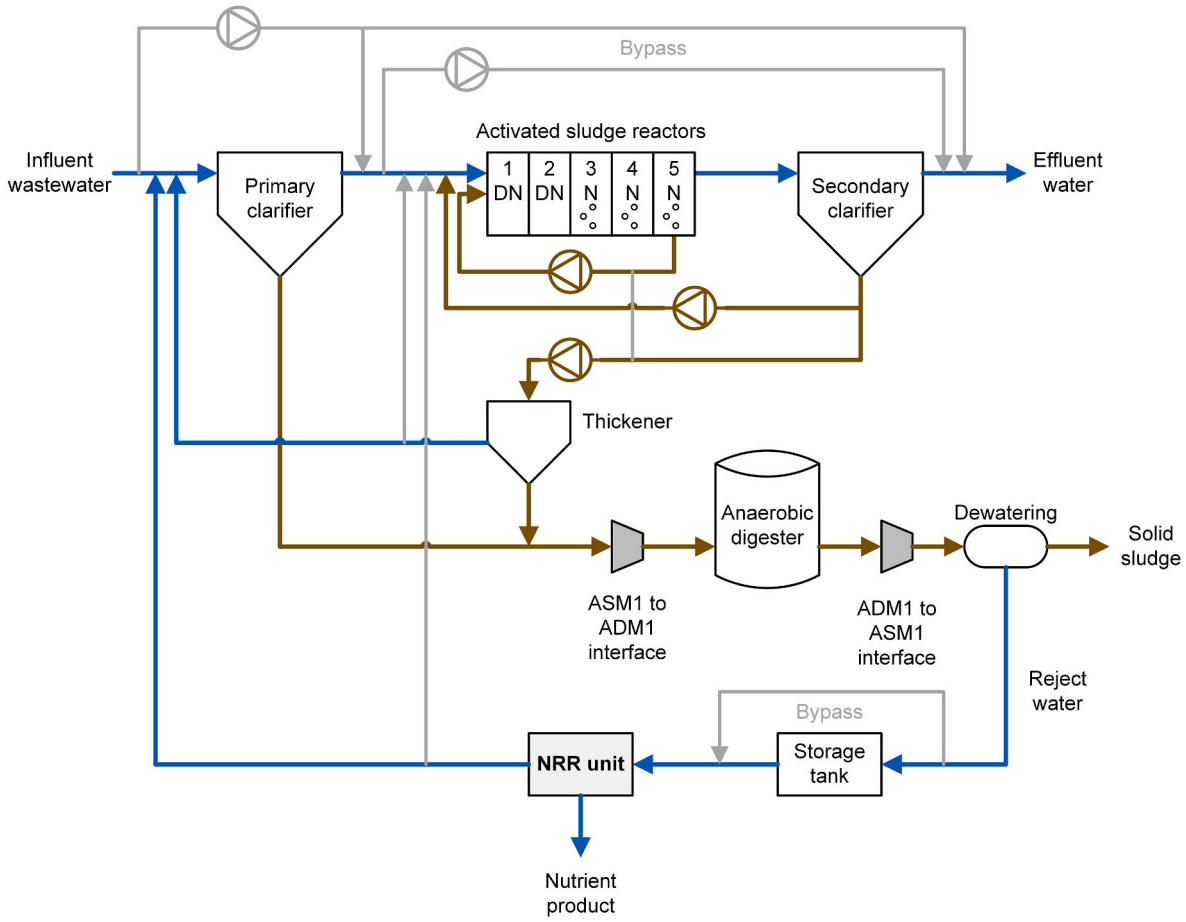

Fig. 1. Schematic diagram of the Benchmark Simulation Model No. 2 (BSM2), modelling a conventional wastewater treatment plant (WWTP). The activated sludge process is divided into an anaerobic denitrification (DN) stage (reactors 1 and 2) and aerated nitrification (N) stage (reactors 3, 4 and 5). Reject water refers to the liquid fraction originating from the dewatering of the digested sewage sludge and the nitrogen removal and recovery (NRR) unit is added in its recirculation line. The blue and brown lines represent the main water and sludge flows within the WWTP, respectively. The grey lines represent the bypasses that are used if needed, i.e., if the loads to the different unit processes become too high, as built into the BSM2. ASM1 = Activated Sludge Model No. 1; ADM1 = Anaerobic Digestion Model No. 1. (For interpretation of the references to colour in this figure legend, the reader is referred to the Web version of this article.)

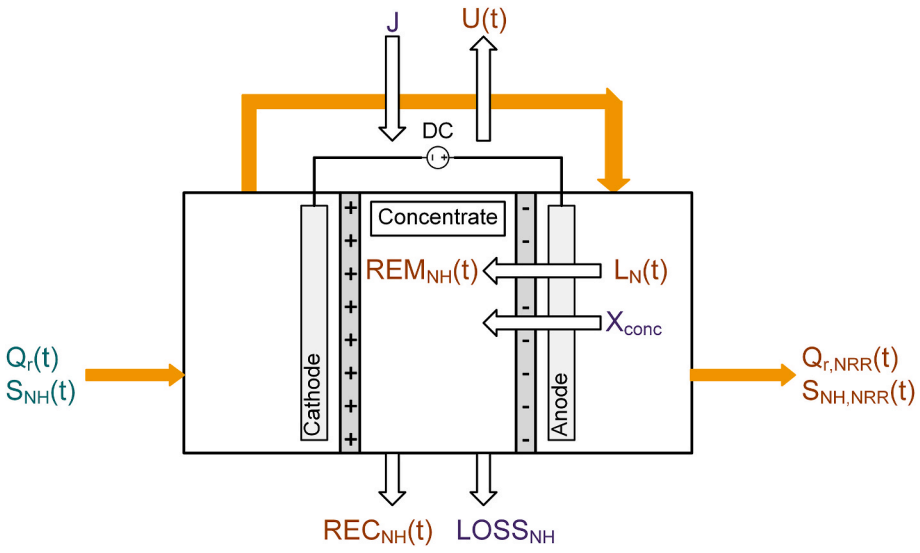

Fig. 2. A simplified schematic presentation of the (bio)electroconcentration ((B)EC) unit used for nitrogen removal and recovery (NRR). The yellow lines represent the reject water flowing through the system. The input functions from storage tank (in green), functions calculated in the NRR unit model (in orange), and constant values (in purple) are presented in different colours. $Q_r(t)$ = influent reject water flow rate; $S_{NH}(t)$ = NH_4–N concentration in influent reject water; J = current density; U(t) = cell voltage; $L_N(t)$ = NH_4–N load ratio; X_{conc} = fractional concentrate production rate; $REM_{NH}(t)$ = nitrogen removal efficiency; $REC_{NH}(t)$ = nitrogen recovery efficiency; $LOSS_{NH}$ = fractional nitrogen loss; $Q_{r,NRR}(t)$ = NRR unit effluent flow rate; $S_{NH,NRR}(t)$ = NH_4–N concentration in the NRR unit effluent. (For interpretation of the references to colour in this figure legend, the reader is referred to the Web version of this article.)

reject water flow (Q_r) and the NH_4–N content of reject water (S_{NH}; Fig. 2), which changed over the simulation time of the model. Note that for simplicity, the notation *NH* is used in the equations and variables to represent NH_4–N. The other ASM1 state variables were assumed to remain unaffected by the NRR unit. The main principle of the NRR unit model was to determine the NH_4–N removal and recovery efficiencies

based on the changing NH_4–N load ratio (L_N) that can be calculated as follows (Rodríguez Arredondo et al., 2017):

$$\boldsymbol{L_N(t)} = \frac{\boldsymbol{J}}{\boldsymbol{S_{NH}(t)} \times \boldsymbol{Q_r(t)} \times \frac{F}{A_m}} \quad (1)$$

where J is the applied current density (A m^{-2}), S_{NH} is the NH_4–N concentration in the reject water (mol m^{-3}), Q_r is the reject water flow rate (m^3 s^{-1}) and F is the Faraday constant (96 485 s A mol^{-1}). The chosen approach was to set the applied current density J at a fixed value, and as a result, the value of L_N changed with the changing Q_r and S_{NH} according to Eq. (1). Based on the laboratory-scale experiments (Koskue et al., 2021a, 2021b), the fractional NH_4–N removal had been found to increase linearly with increasing L_N (in a certain L_N range; Figs. S4 and S6 in Supplementary Material). Thus, the fractional NH_4–N removal X_{NH} was calculated from the L_N using the experimentally determined linear fitting coefficients p1 and p2:

$$\boldsymbol{X_{NH}(t)} = \boldsymbol{p1} \times \boldsymbol{L_N(t)} + \boldsymbol{p2} \quad (2)$$

The linear fitting coefficients for the BEC-NRR and the EC-NRR are presented in Table S3. All used coefficients had a value between 0 and 1. X_{NH} was further limited to a maximum value of 0.94 based on the maximum removal efficiency 94.4 ± 0.7% observed in the laboratory-scale experiments (Koskue et al., 2021a). As the laboratory-scale experiments had shown, the NH_4–N removal responded dynamically to changes in the influent conditions before reaching steady-state. The mass of the removed NH_4–N was modelled using the fractional removal X_{NH}, influent reject water characteristics, and a parameter τ as:

$$\boldsymbol{\tau} \times \frac{\boldsymbol{d}}{\boldsymbol{dt}}\boldsymbol{REM_{NH}(t)} = \boldsymbol{X_{NH}(t)} \times \boldsymbol{S_{NH}(t)} \times \boldsymbol{Q_r(t)} - \boldsymbol{REM_{NH}(t)},\ \boldsymbol{REM_{NH}(0)} \quad (3)$$

where $\tau = 1$ (d) is the value of the experimentally determined time constant that estimates the response time of the NH_4–N removal, and $REM_{NH}(0)$ is the initial mass of NH_4–N in the concentrate chamber. More details on the dynamic modelling can be found in Appendix A and Figs. S8–S9 in the Supplementary material. Note that in case of a steady-state situation, the removed NH_4–N is given by $\overline{REM_{NH}} = \overline{X_{NH}} \times \overline{S_{NH}} \times \overline{Q_r}$, where $\overline{REM_{NH}}$, $\overline{X_{NH}}$, $\overline{S_{NH}}$, and $\overline{Q_r}$ are the steady-state values of the NRR functions.

As experienced in the laboratory-scale experiments (Koskue et al., 2021a, 2021b), not all of the removed NH_4–N can be effectively recovered as losses occur in systems due to, e.g., volatilisation or electrochemical oxidation. Therefore, the recovered NH_4–N (REC_{NH}) was always slightly lower than the REM_{NH}, expressed using the empirically determined fractional NH_4–N loss ($LOSS_{NH}$):

$$\boldsymbol{REC_{NH}(t)} = (1 - \boldsymbol{LOSS_{NH}}) \times \boldsymbol{REM_{NH}(t)} \quad (4)$$

Based on the laboratory-scale results, $LOSS_{NH}$ was fixed at a constant value of 0.05 for the BEC-NRR and 0.1 for the EC-NRR.

As the NH_4–N removal/recovery took place via the generation of a nitrogen-rich liquid stream, the NRR unit also caused a slight reduction to the volumetric flow of the reject water (Q_r). As the applied current was kept constant, leading to a constant electro-osmotic force, the generation rate of the liquid concentrate (X_{conc}) was fixed at 0.025 of the influent flow for the BEC-NRR and 0.035 for the EC-NRR based on the laboratory-scale observations (Koskue et al., 2021a, 2021b). The reduced reject water flow rate from the NRR unit that circulated back to the wastewater treatment process was therefore calculated as:

$$\boldsymbol{Q_{r,NRR}(t)} = (1 - \boldsymbol{X_{conc}}) \times \boldsymbol{Q_r(t)} \quad (5)$$

According to the experiments, the dynamic behaviour of nitrogen removal is much slower (a few days) than the change in water flow rates (a few hours). Therefore, it was not useful to model the volumetric change (Eq. (5)) using a differential equation. Furthermore, the NH_4–N removal by the NRR unit resulted in a lower NH_4–N concentration in the unit output:

$$\boldsymbol{S_{NH,NRR}(t)} = \frac{(1 - \boldsymbol{X_{NH}(t)}) \times \boldsymbol{S_{NH}(t)} \times \boldsymbol{Q_r(t)}}{\boldsymbol{Q_{r,NRR}(t)}} = \frac{\boldsymbol{S_{NH}(t)} \times \boldsymbol{Q_r(t)} - \boldsymbol{REM_{NH}(t)}}{\boldsymbol{Q_{r,NRR}(t)}},\ \boldsymbol{S_{NH,NRR}(0)} \quad (6)$$

where $S_{NH,NRR}(0)$ is the initial value of the NH_4–N concentration in the NRR output stream. The simulation model was implemented so that $S_{NH,NRR}(0) = S_{NH}(0)$. The simulated responses of REC_{NH}, $S_{NH,NRR}$ and $Q_{r,NRR}$ with constant influent reject water characteristics are presented in Figs. S10–S12.

2.3. Simulations

Three different sets of simulations were run: 1) a control simulation, where the BSM2 was operating without the NRR unit; 2) simulations with the BEC-NRR unit; and 3) simulations with the EC-NRR unit. The BEC-NRR and EC-NRR simulation sets were further divided into three individual simulations: low performance, base case, and high performance (Table 1). In these simulations, all the other BEC-NRR- and EC-NRR-specific model parameter values were maintained constant, but the current density was varied. The base case simulation represented a current density value considered most realistic based on the laboratory experiments (Koskue et al., 2021a, 2021b). The low and high performance simulations used current densities from the lower and upper end, respectively, of the potential current density range.

2.4. Control strategy and evaluation criteria

The control strategy implemented in the BSM2 + NRR model involved controlling both the aeration and external carbon addition of the activated sludge process. First, the aeration of the activated sludge process was controlled using the default control strategy of the BSM2 (Gernaey et al., 2014), i.e., maintaining the dissolved oxygen concentration in the fourth bioreactor at 2 g_{O2} m^{-3}. Second, the external carbon dosage to the first anaerobic bioreactor was manipulated to maintain the nitrate (S_{NO}) level of the second bioreactor at a defined set-point (1 $g_{NO3\text{-}N}$ m^{-3}), as done previously (Volcke et al., 2006). Details can be found in Appendix A of the Supplementary Material. It should be noted that the focus of the study was not to optimise the control strategy but to use a same strategy for all simulations to assess the effects of the altered nitrogen load on the aeration and external carbon addition requirements.

According to the BSM2 guidelines, all seven simulations were run for a total of 609 days and the evaluations based on the average values during the final 365 days of the simulations (Alex et al., 2018; Gernaey et al., 2014). The changes in the WWTP effluent water quality were assessed by looking at the individual average concentrations of selected key parameters in the effluent as well as the overall effluent quality index (EQI). The EQI was calculated as a weighted sum of relevant effluent concentrations, namely the total suspended solids (TSS),

Table 1
A summary of the simulations run with and without the nutrient removal and recovery (NRR) unit.

Simulation set	No. of simulations	Applied current density for the NRR unit [A m^{-2}]		
		Low performance	Base case	High performance
Control	1	n.a.	n.a.	n.a.
BEC-NRR	3	1	5	10
EC-NRR	3	5	35	70

n.a. = not applicable.

chemical oxygen demand (COD), biological oxygen demand (BOD_5), and the total nitrogen, as previously detailed (Copp, 2002). For the total nitrogen and NH_4–N, the BSM2 effluent limit concentrations of 18 g m^{-3} and 4 g m^{-3}, respectively, were used (Alex et al., 2018; Gernaey et al., 2014). Furthermore, the BSM2 operational cost index (OCI) was used as an indicator of the changes in the OPEX between the simulations (Alex et al., 2018; Gernaey et al., 2014). The OCI was calculated as a weighted sum of operational cost factors, including the additional electrical energy used by the NRR unit, as detailed in Appendix A of the Supplementary Material.

2.5. Economic analysis

2.5.1. Detailed treatment cost analysis

The OCI built into the BSM2 is not designed to take into account the generation of an additional product with a monetary value, i.e., the nitrogen-rich liquid nutrient product. Nor does it consider the additional capital CAPEX required for the implementation of the NRR unit into an existing WWTP. Therefore, a more comprehensive economic analysis was conducted.

The OPEX of the combined wastewater and sludge treatment process include the electrical energy used for aeration, pumping, mixing and the NRR unit, the heating energy used in the AD, the external carbon addition and the sludge production for disposal. The generated products with additional value include methane and the liquid nutrient product. As detailed later in Section 3.1.3, the changes in pumping and mixing energy, heating energy, sludge production and methane production were minor (≤5%) between the different simulations, and therefore deemed insignificant for the comparison of the OPEX. Therefore, the OPEX analysis focused on the energy used for aeration and the NRR unit, and the external carbon addition. Furthermore, the estimated revenue of the nutrient product was included. The average yearly costs/revenue related to each of these four items were calculated by multiplying the average yearly amount used/generated (Tables 3 and 5) by an estimated unit price (Table 2). The yearly costs and revenue were further normalised to the total volume of wastewater treated, based on the average influent flow of 20 648 m^3 d^{-1} (Gernaey et al., 2014).

The CAPEX were largely based on unit prices and life time assumptions used previously (Jourdin et al., 2020; Rozendal et al., 2008). The total CAPEX are presented in Table 2 and detailed in Table S5. As detailed cost data are currently scarce due to the technology only being implemented in laboratory-scale, the used values are educated guesses and represent a slightly optimistic scenario where the materials are available in bulk (Jourdin et al., 2020). The CAPEX per year were calculated by distributing the total investment over the estimated lifetime of each item and normalised to the average yearly volume of wastewater treated, as done for the OPEX and revenue. The CAPEX of the full WWTP were not considered here, as the assumption was that the WWTP already existed. The overall treatment cost (per m^{-3}) for each scenario was calculated by reducing the CAPEX and OPEX from the expected revenue.

Table 2
The values used in the sensitivity analysis.

		Minimum	Median	Maximum
CAPEX	BEC-NRR [EUR $year^{-1}$]	32697	65395[a]	653947
	EC-NRR [EUR $year^{-1}$]	37565	75131[a]	751309
OPEX	Electricity [EUR kWh^{-1}]	0.06415	0.1283[b]	0.19245
	External carbon [EUR kg_{COD}^{-1}]	0.2525	0.505[c]	0.7575
Revenue	Nutrient product [EUR kg_N^{-1}]	2[d]	20	100[e]

[a] Detailed itemisation is presented in Table S5 in Supplementary Material.
[b] Average electricity price for non-household customers in the European Union during the first half of 2021 (Eurostat, 2022).
[c] Regional contract price provided by the largest methanol supplier in the world, Methanex, for Europe in January–March 2022 (Methanex, 2022).
[d] Average price for industrially produced nitrogen fertilisers on the second week of January 2022 (DTN, 2022).
[e] Based on the retail price of commercial liquid fertilisers with a similar nitrogen concentration, as detailed in Table S6.

Table 3
Average ammonium nitrogen (NH_4–N) load ratios and resulting NH_4–N removal efficiencies and recovery yields obtained in the different simulations during the evaluation period, i.e., the final 365 d of the simulation.

	BEC-NRR			EC-NRR		
	Low	Base	High	Low	Base	High
Average NH_4–N load ratio, L_N [-]	0.06	0.31	0.62	0.31	2.23	4.50
Average NH_4–N removal efficiency [%]	33	39	47	58	80	92
Average NH_4–N recovery [kgN d^{-1}]	79	94	111	132	178	204

To determine whether a scenario would be profitable throughout its entire lifetime, net present value (NPV) was used to discount future cash flows to the present value. The NPV was thereby selected as the profitability indicator for comparing the different scenarios and calculated using a design horizon of 25 years (Rozendal et al., 2008) and a discount rate of 5% (Jourdin et al., 2020; Kwan et al., 2018) as follows:

$$NPV = \sum_{t=1}^{T} \frac{C_t}{(1+d)^t} - C_0 \quad (7)$$

where $t = 25$ is the design horizon (years), C_t is the net cash flow during period t (EUR m^{-3}), $d = 5$ is the discount rate (%), and C_0 is the initial investment (EUR m^{-3}). Ct was calculated by reducing the OPEX from the nutrient product revenue.

2.5.2. Sensitivity analysis

The impact of different variables on the treatment cost obtained in each simulation scenario was evaluated through a sensitivity analysis. A number of variables were set at alternating variation of their median value one at a time to study their significance on the overall treatment cost. The variables being alternated included CAPEX, OPEX, and nutrient product value (Table 2). As the median CAPEX value could be considered optimistic (see Section 2.5.1), the maximum value for the sensitivity analysis was set at ten times as high. The minimum CAPEX value was set at 50% of the median value. For the OPEX, the cost for both electricity and external carbon addition as methanol were set at ±50% variation of their median value, an approach used before (Kwan et al., 2018).

For the nutrient product, the minimum value was set at the current price for industrially synthesised fertiliser nitrogen (DTN, 2022). The maximum value was based on the value calculated for commercial liquid fertilisers marketed for household use as EUR kg_N^{-1} based on their nitrogen content, product size and price (Table S6). The prices per kg_N varied quite notably from ca. 100 to >2000 EUR kg_N^{-1} (Table S6), and the maximum value for the sensitivity analysis was set at a value from the lower end of the price range. Finally, the median value for the nutrient product price was set at 20% of the maximum value, based on the assumption that the nutrient product could be sold at 20% of its retail value.

3. Results and discussion

3.1. Simulation results

3.1.1. Nitrogen removal and recovery

The influent reject water characteristics remained almost identical in all the NRR simulations (with the NH_4–N concentrations varying between 1300 and 1600 g m^{-3}), the main parameter determining the obtained nitrogen load ratio was the current density (Eq. (1)). The higher current densities applied for the EC-NRR (Table 1) also led to

Table 4
Effluent quality in terms of total nitrogen and NH_4–N for the different simulations.

		Control	BEC-NRR			EC-NRR		
			Low	Base	High	Low	Base	High
Total nitrogen (effluent limit 18 g m^{-3})	95% percentile [g_N m^{-3}]	14.5	13.5	13.3	13.1	12.7	12.1	11.8
	% of time limit violation [%]	0.22	0	0	0	0	0	0
	No. of limit violations [-]	8	0	0	0	0	0	0
NH_4–N (effluent limit 4 g m^{-3})	95% percentile [g_N m^{-3}]	1.7	1.8	1.8	1.9	1.9	1.9	1.9
	% of time limit violation [%]	0.6	0.5	0.5	0.5	0.5	0.5	0.5
	No. of limit violations [-]	16	14	14	15	17	18	19

Table 5
Average daily consumption of selected operational parameters in the different simulations.

	Control	BEC-NRR			EC-NRR		
		Low	Base	High	Low	Base	High
Average aeration energy [kWh d^{-1}]	4390	4104	4051	3985	3881	3705	3605
Average NRR unit energy [kWh d^{-1}]	n.a.	3639	15683	24885	38992	493526	1363273
External carbon addition [kg_{COD} d^{-1}]	1493	1131	1059	970	830	596	469

n.a. = not applicable.

higher NH_4–N load ratios, and consequently to higher NH_4–N removal efficiencies (Table 3 and Fig. S13). With the BEC-NRR, the NH_4–N removal efficiencies remained below 50%, the highest efficiency being 47% in the BEC–high scenario. With the EC-NRR, on the other hand, almost complete removal of 92% was obtained in the EC–high scenario.

The average NH_4–N recoveries ranged between 79 and 111 kg_N d^{-1} for the BEC-NRR and 132–204 kg_N d^{-1} for the EC-NRR (Table 3). On a yearly basis, these would translate to ca. 29–74 t_N $year^{-1}$.

3.1.2. Effluent quality

As the implemented NRR unit reduced the NH_4–N load in the reject water returned to the wastewater treatment process, special focus was paid to the effect this had on the nitrogen in the treated WWTP effluent water (Table 4 and Fig. S14). The effect was especially notable on the total nitrogen content of the effluent. The 95% percentile, i.e., the concentration that was exceeded only 5% of the simulation time, for total nitrogen was reduced from the 14.5 g_N m^{-3} in the control run to 13.1–13.5 g_N m^{-3} (corresponding to a 7–10% percentual decrease) with the BEC-NRR and to 11.8–12.7 g_N m^{-3} (12–19% reduction) with the EC-NRR. At the same time, the effluent limit of 18 g_N m^{-3} for total nitrogen was not violated once when the NRR unit was in use, compared to eight individual violations, corresponding to 0.22% of the overall evaluation period, in the control run.

Interestingly, the 95% percentile for NH_4–N slightly increased in all the simulations including the NRR unit compared to the control (Table 4). Furthermore, the number of effluent limit (4 g_N m^{-3}) violation events increased from 16 in the control to 17–19 with the EC-NRR, while the BEC-NRR achieved slightly lower values of 14–15. Nevertheless, the time the effluent limit was violated compared to the overall simulation time was lower at ca. 0.5% with all the NRR unit simulations compared to the 0.6% in the control. The slight increases in the effluent NH_4–N concentrations suggest that the reductions in the total nitrogen content of the effluent water were due to better removal of other nitrogen species in the wastewater treatment process. Indeed, when looking at the average effluent concentrations, the nitrate and nitrite nitrogen (NO_x-N) concentration decreased by ca. 10–14% with the BEC-NRR and 17–27% with the EC-NRR compared to the control, which was a consequence of keeping the internal recycle flow rate from the last aerobic tank to the first anoxic tank constant. At the same time, the NH_4–N concentrations increased by ca. 3–5% with the BEC-NRR and 6–12% with the EC-NRR. A potential explanation for this are the observed decreases in both the heterotrophic (up to 14% reduction) and autotrophic (up to 25% reduction) biomass growth in the activated sludge reactors. The NO_x-N, which was removed more efficiently, was potentially limiting the biomass growth, which resulted in slightly lower NH_4–N removal in the activated sludge process. This suggests the applied control strategy was more efficient in optimising NO_x-N removal over NH_4–N removal, and changes to the strategy could be considered to minimise the NH_4–N concentration in the effluent.

When converting the total nitrogen concentrations in the effluent water to average daily loads to the receiving water bodies, the load of 223 kg_N d^{-1} with the control was reduced to 199–205 kg_N d^{-1} with the BEC-NRR and 177–193 kg_N d^{-1} with the EC-NRR. On a yearly basis, the average total nitrogen load of ca. 81 t_N $year^{-1}$ in the control case would be reduced by ca. 6–9 t_N $year^{-1}$ with the BEC-NRR and further by 11–17 t_N $year^{-1}$ with the EC-NRR. As eutrophication is an issue in many water systems and WWTP discharge limits have therefore become more and more stringent in recent years, WWTPs are potentially facing changes to their operation to achieve higher removal efficiencies and better effluent quality. Retrofitting a (B)EC-NRR unit into the reject water circulation line might be a feasible option to realise the ca. 10–20% reduction in nitrogen release without the need to expand the plant size.

In addition to the individual compound concentrations and loads, the overall EQI (expressed as pollutant units per day, kg_{PU} d^{-1}) was reduced, i.e., the effluent quality improved in all the NRR unit simulations

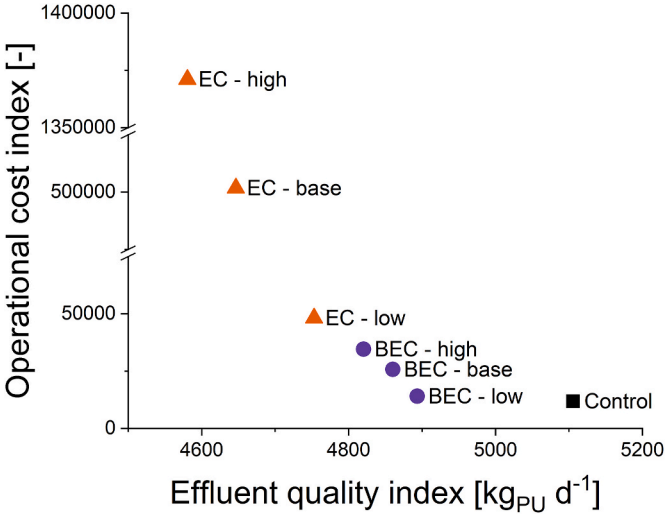

Fig. 3. Presentation of the two evaluation criteria, the operational cost index (calculated according to Eq. S3) and effluent quality index, for the different simulations.

compared to the control (Fig. 3). The improvement was ca. 4–6% with the BEC-NRR and 7–10% with the EC-NRR. This was largely due to the reduced total nitrogen concentration in the effluent, but minor decreases for the TSS (2–5% reduction), COD (1–2%) and BOD_5 (3–8%) concentrations were also observed in all the simulations including the NRR unit.

3.1.3. Operational cost index

In addition to the changes in the effluent quality, another key evaluation criterium for comparing the simulations was the OCI (Eq. S3). While the NRR unit reduced both the aeration energy and external carbon addition requirement in all six cases (Fig. 4 and Fig. S15), the additional electric energy consumed by the NRR unit negated these reductions and increased the total OCI in all studied scenarios (Figs. 3 and 4). In the BEC–low case, the increase in the OCI was the lowest at 18% higher than in the control, while the EQI was simultaneously improved by 4%. All the other scenarios more than doubled the OCI compared to the control case.

The changes between simulations remained at ≤5% for all other cost segments except for the aeration energy and external carbon addition, in addition to the energy consumed by the NRR unit (Fig. 4). This is expected as the implemented control strategy (Section 2.4) specifically focused on controlling the aeration and the carbon dosage. The EC–high scenario resulted in the highest reductions in both the external carbon addition (71%) and aeration energy (19%) compared to the control (Table 5 and Fig. S15). However, as mentioned previously, the additional electrical energy cost required to achieve these reductions was extremely high at >1 GWh d^{-1}. The BEC–low scenario with a considerably more moderate energy consumption for the NRR unit reduced the carbon dosage by 24% and the aeration energy by 7%. Generally, the reductions in the aeration energy and carbon addition increased with increasing NH_4–N removal efficiency but at the same time the overall energy cost of the scenario increased due to the higher applied current densities in the NRR unit.

As mentioned in Section 2.4, the model ignored the potential increase in pumping and mixing energy caused by the NRR unit. In reality, mixing of the anode and cathode chambers would likely be required to reduce mass transfer limitations and obtain the assumed nitrogen removal efficiencies, as done in the laboratory experiments (Koskue et al., 2021a, 2021b). In the BSM2 model, however, the pumping and mixing energy requirements on the full WWTP scale were found order(s) of magnitude lower than the aeration energy, carbon dosage and the energy demand of the NRR unit (Fig. 4). Therefore, the additional mixing energy requirements can be expected to have little or no significance to the OCI.

A previous study assessed the effect of nitrogen removal from reject water with a combination of SHARON-Anammox, using a preliminary version of the BSM2 (Volcke et al., 2006). The SHARON-Anammox reduced the OCI by 13% compared to the unmodified BSM2, simultaneously improving the overall effluent quality by 18%. The reduction in the OCI was mainly due to the significant (95%) decrease in the external carbon requirement, while more NH_4–N was also removed at a similar aeration energy consumption compared to the control. It should, however, be noted that the nitrogen was removed from the reject water stream as N_2 gas and not recovered in a reusable form, as in this study.

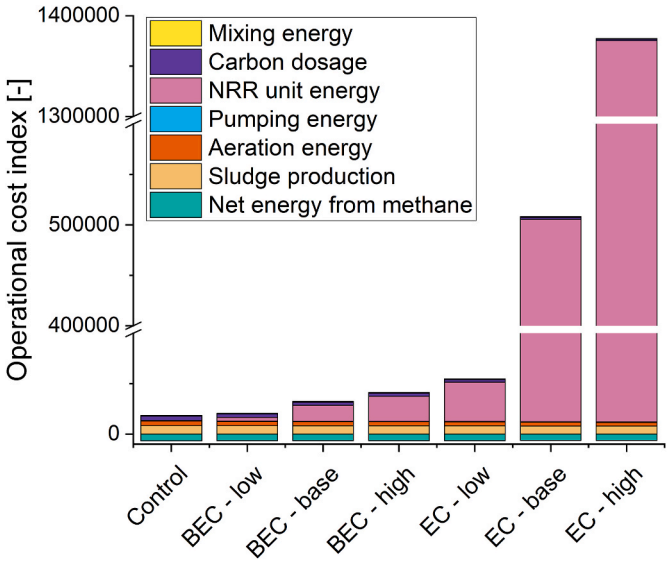

Fig. 4. The operational cost indices presented by segment for the different simulations. The values for the net energy from methane are negative (according to Eq. S3) as methane production generates energy in the process instead of consuming it.

3.2. Economic evaluation

3.2.1. Comparison of the different scenarios

The detailed cost analysis focused on the CAPEX of the NRR unit, the electrical energy consumed by aeration and the NRR unit, the external carbon addition, and the revenue from the generated nutrient product (see Section 2.5.1). The NPV (Eq. (7)) was used for comparing the different scenarios (Fig. 5, with a positive NPV generally indicating profitability. More specifically, in this study, a positive NPV suggests a net profit from wastewater treatment. However, an equally important threshold is the NPV of the control scenario, as scenarios reaching an NPV higher than the control can be considered economically attractive compared to the business-as-usual.

The NPV for the control scenario was calculated as −9.5 EUR m^{-3} (Fig. 5). The two BEC-NRR scenarios using the lowest current densities, 1 and 5 A m^{-2}, obtained NPVs higher than this, making them economically more attractive compared to the control case. The BEC–base scenario resulted in a slightly higher NPV (−8.6 EUR m^{-3}) than the control, whereas the BEC–low scenario actually obtained a positive NPV (0.1 EUR m^{-3}), indicating a net profit instead of a treatment cost. The NPVs

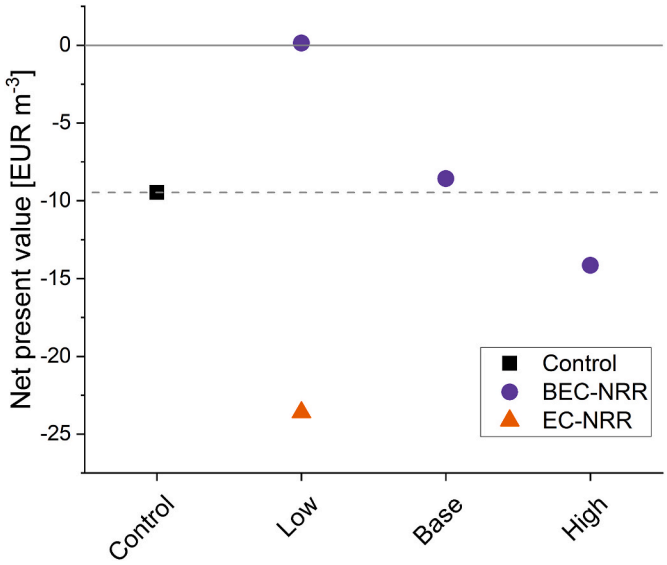

Fig. 5. The net present value (NPV) per volume of wastewater treated (EUR m^{-3}) calculated for the different scenarios: the control without the nitrogen removal and recovery (NRR) unit, the scenarios using the bio-electroconcentration (BEC)-NRR unit (low, base and high), and one scenario using the electroconcentration (EC)-NRR unit (low). The EC–base and EC–high scenarios were excluded from the graph for having NPVs order(s) of magnitude lower (−435 and −1232 EUR m^{-3}, respectively), making them far from feasible.

of the other NRR scenarios were not competitive with the NPV of the control.

The results indicate that the BEC-NRR with a lower energy consumption compared to the EC-NRR could be a viable option in reducing the water treatment costs of an existing WWTP. Alternatively, the inclusion of an NRR unit for reject water treatment could be considered already in the planning and constructing of a completely new WWTP. In this case, the reduced nitrogen load to the activated sludge process could result in a reduced bioreactor volume requirement and thus lower CAPEX. The dimensioning of the activated sludge process is largely based on the estimated biomass generation rate and sludge retention time (SRT). Typically, the oxidation of NH_4–N in the nitrification stage of the activated sludge process is the rate limiting step, and thereby determines the SRT and the activated sludge process volume (Metcalf and Eddy, 2014). The observed reductions in the active heterotrophic and autotrophic biomasses were at the highest 7% and 15%, respectively, using the BEC-NRR, which gives an estimate on the degree of the potential size reduction for the activated sludge process.

3.2.2. *Factors affecting NRR unit feasibility*

The sensitivity analysis conducted for the treatment costs (as detailed in Section 2.5.2) revealed that the trade price for the nutrient product affected the cost of the treatment to the greatest extent in most of the studied scenarios (Fig. 6 and Fig. S16). In the EC-base and EC-high scenarios, the electricity demand of the NRR unit was so high that the electricity price started to cause the greatest fluctuation in the treatment cost (Fig. S16). The CAPEX were found to be a notable contributor to the treatment costs at the low current densities of the BEC–low and BEC–base scenarios (Fig. 6), but became inferior to the variation in the electricity price in the scenarios using higher current densities.

The results of the sensitivity analysis suggest that the viability of the proposed NRR unit largely depends on the market and expected revenue for the generated nutrient product. As mentioned in Section 1, the nitrogen fertiliser prices have been on the rise and are expected to increase in the future, which is promising for the potential implementation of the technology. On the other hand, this dependency on the nutrient product value makes the technology susceptible to market fluctuations, with little control over the nitrogen retail price. From a technology-optimisation point of view, the results clearly indicate that the energy consumption of especially the EC-NRR needs to be lowered to make it a viable alternative for realising nitrogen recovery.

3.3. *Model limitations and outlook*

The NRR unit simulations conducted in this study were based on limited empirical data from laboratory-scale experiments and several assumptions and simplifications were made with no attempt to model the actual (bio)chemical reactions taking place in the NRR unit. Therefore, the results presented here are a rough first estimation and cannot be generalised for other (bio)electrochemical nutrient recovery methods. The results clearly reveal, however, that the key factor in making a (B)EC system feasible in larger scale is minimising its energy consumption. For minimising the (B)EC energy requirement, further optimisation of the operational set-up, e.g., via the implementation of air-cathodes, should be conducted in laboratory-scale. Furthermore, instead of applying a constant current density, an automated control of the current density applied into the NRR unit based on the fluctuating NH_4–N load could be developed to keep the NH_4–N load ratio at the most energy-efficient level.

The NRR unit was also expected to have no effect on the other ASM1 state variables except for the S_{NH} and Q_r. In reality, decreases in, e.g., the organic matter can be expected (Koskue et al., 2021a, 2021b). However, this decrease in the COD is not significant for the carbon to nitrogen ratio in the activated sludge process, as the contribution of the COD in the reject water flow to the overall COD load to the activated sludge process (ca. 1%) is much lower compared to the NH_4–N (ca. 35% in the control simulation).

The used BSM2 also has its own limitations. For one, the model does not consider several other soluble compounds of interest for the NRR unit, such as potassium, sodium and chloride. Instead of the nitrogen load ratio used in this study, the combined cation load ratio was recently identified as a better indicator of the expected (B)EC performance (Koskue et al., 2021a). However, with the information for the other cations in the reject water lacking from the BSM2, the simpler nitrogen load ratio had to be used here. The identified main model limitations are also visually summarised in Fig. S17.

So far, generic large-scale models dedicated to nitrogen recovery have been scarce and only a few models have been developed for nutrient recovery strategies identified as the most established, including precipitation/crystallisation, stripping and acidic air scrubbing (Vaneeckhaute et al., 2018). In the future, advances in system optimisation and experimental trials in larger scale will hopefully facilitate the development and validation of increasingly accurate (bio)electrochemical nitrogen recovery models.

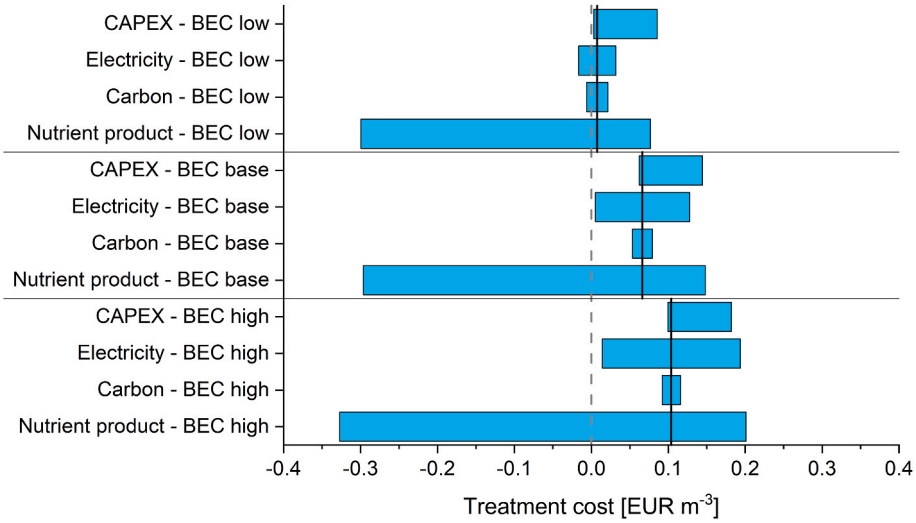

Fig. 6. Sensitivity analysis results for the scenarios using the bioelectroconcentration (BEC)-NRR: low, base and high. The solid vertical lines represent the median value cases. The dashed vertical line represents a treatment cost of 0 EUR m^{-3} and negative values mean a net profit. Sensitivity analysis results for the electroconcentration (EC)-NRR scenarios can be found in Fig. S16 in the Supplementary Material.

4. Conclusions

This study assessed the technoeconomic feasibility of integrating a (B)EC-NRR into a full-scale WWTP for nitrogen removal and recovery from the reject water circulation line through modelling. In all the modelled scenarios, nitrogen removal and recovery from reject water was found to improve the WWTP effluent quality compared to the control, especially considering the total nitrogen concentration. An applied current density as low as 1 A m^{-2}, leading to a NH_4–N removal efficiency of 32.6%, was enough to completely prevent violations of the effluent limit (18 g m^{-3}) for total nitrogen. Higher applied current densities increased the nitrogen removal and recovery efficiencies up to 92%, which consequently led to larger reductions in aeration energy (up to 19%) and external carbon dosage (up to 71%) in the activated sludge process. At the same time, however, the additional energy consumed by the NRR unit also increased and negated the savings in other parts of the treatment process. As a result, the total OPEX increased in all scenarios using the NRR unit by ≥18%, but the expected revenue from the generated nutrient product was enough to make the BEC-NRR scenario using the lowest current density (1 A m^{-2}) net-profitable and the scenario using 5 A m^{-2} also economically attractive compared to the control. The sensitivity analysis revealed that the nutrient product value had the largest impact on the economics of almost all studied scenarios, whereas the electricity price played the most notable role in the scenarios with the highest energy consumption due to the higher applied current densities (up to 70 A m^{-2}).

Credit author statement

Veera Koskue: Conceptualization, Methodology, Investigation, Formal analysis, Visualization, Writing – original draft, Funding acquisition. **Veli-Pekka Pyrhönen**: Methodology, Visualization, Writing – review & editing. **Stefano Freguia**: Conceptualization, Methodology, Supervision, Writing – review & editing. **Pablo Ledezma**: Conceptualization, Methodology, Supervision, Writing – review & editing. **Marika Kokko**: Conceptualization, Methodology, Supervision, Writing – review & editing.

Funding

This work was supported by Tampere University supporting Veera Koskue. Pablo Ledezma acknowledges a Research Stimulus Fellowship from The University of Queensland.

Declaration of competing interest

The authors declare that they have no known competing financial interests or personal relationships that could have appeared to influence the work reported in this paper.

Appendix A. Supplementary data

Supplementary data to this article can be found online at https://doi.org/10.1016/j.jenvman.2022.115747.

References

Alex, J., Benedetti, L., Copp, J., Gernaey, K., Jeppsson, I., Nopens, I., Pons, M., Rosen, C., Steyer, J., Vanrolleghem, P., 2018. Benchmark simulation model no. 2 (BSM2). Water Sci. Technol. 2, 1–99.

Copp, J.B., 2002. The COST Simulation Benchmark: Description and Simulator Manual.

Daigger, G.T., 2014. Oxygen and carbon requirements for biological nitrogen removal processes accomplishing nitrification, nitritation, and Anammox. Water Environ. Res. 86, 204–209. https://doi.org/10.2175/106143013x13807328849459.

Desloover, J., Woldeyohannis, A.A., Verstraete, W., Boon, N., Rabaey, K., 2012. Electrochemical resource recovery from digestate to prevent ammonia toxicity during anaerobic digestion. Environ. Sci. Technol. 46, 12209–12216. https://doi.org/10.1021/es3028154.

DTN, 2022. DTN Retail fertilizer trends [WWW Document]. Progress. Farmer. URL. https://www.dtnpf.com/agriculture/web/ag/crops/article/2022/01/19/fertilizer-prices-continue-mostly. accessed 2.10.22.

DTN, 2021. Global fertilizer outlook - 1 [WWW Document]. Progress. Farmer. URL. https://www.dtnpf.com/agriculture/web/ag/crops/article/2021/12/13/world-nitrogen-demand-increase-2022. accessed 2.10.22.

Erisman, J.W., Sutton, M.A., Galloway, J., Klimont, Z., Winiwarter, W., 2008. How a century of ammonia synthesis changed the world. Nat. Geosci. 1, 636–639. https://doi.org/10.1038/ngeo325.

Eurostat, 2022. Electricity price statistics. In: Electricity Prices for Non-household Consumers [WWW Document]. URL. https://ec.europa.eu/eurostat/statistics-explained/index.php?title=Electricity_price_statistics#Electricity_prices_for_non-household_consumers. accessed 2.10.22.

Flores-Alsina, X., Ramin, E., Ikumi, D., Harding, T., Batstone, D., Brouckaert, C., Sotemann, S., Gernaey, K.V., 2021. Assessment of sludge management strategies in wastewater treatment systems using a plant-wide approach. Water Res. 190, 116714 https://doi.org/10.1016/j.watres.2020.116714.

Fux, C., Siegrist, H., 2004. Nitrogen removal from sludge digester liquids by nitrification/denitrification or partial nitritation/anammox: environmental and economical considerations. Water Sci. Technol. 50, 19–26. https://doi.org/10.2166/wst.2004.0599.

Gernaey, K.V., Flores-Alsina, X., Rosen, C., Benedetti, L., Jeppsson, U., 2011. Dynamic influent pollutant disturbance scenario generation using a phenomenological modelling approach. Environ. Model. Software 26, 1255–1267. https://doi.org/10.1016/j.envsoft.2011.06.001.

Gernaey, K.V., Rosen, C., Jeppsson, U., 2006. WWTP dynamic disturbance modelling - an essential module for long-term benchmarking development. Water Sci. Technol. 53, 225–234. https://doi.org/10.2166/wst.2006.127.

Gernaey, K.V., Jeppsson, U., Vanrolleghem, P.A., Copp, J.B., 2014. Benchmarking of Control Strategies for Wastewater Treatment Plants, Scientific and Technical Report Series No. 23. IWA Publishing, pp. 1–142.

Giordano, A., Di Capua, F., Esposito, G., Pirozzi, F., 2019. Long-term biogas desulfurization under different microaerobic conditions in full-scale thermophilic digesters co-digesting high-solid sewage sludge. Int. Biodeterior. Biodegrad. 142, 131–136. https://doi.org/10.1016/j.ibiod.2019.05.017.

Guo, H., Yuan, P., Pavlovic, V., Barber, J., Kim, Y., 2020. Ammonium sulfate production from wastewater and low-grade sulfuric acid using bipolar- and cation-exchange membranes. J. Clean. Prod. 285, 124888 https://doi.org/10.1016/j.jclepro.2020.124888.

IFA, 2021. Public Summary. Medium-Term Fertilizer Outlook 2021–2025.

Jaffer, Y., Clark, T.A., Pearce, P., Parsons, S.A., 2002. Potential phosphorus recovery by struvite formation. Water Res. 36, 1834–1842. https://doi.org/10.1016/S0043-1354(01)00391-8.

Jourdin, L., Stralen, N., Van, Strik, D.P.B.T.B., 2020. Techno-economic assessment of microbial electrosynthesis from CO 2 and/or organics : an interdisciplinary roadmap towards future research and application. Appl. Energy 279. https://doi.org/10.1016/j.apenergy.2020.115775.

Koskue, V., Freguia, S., Ledezma, P., Kokko, M., 2021a. Efficient nitrogen removal and recovery from real digested sewage sludge reject water through electroconcentration. J. Environ. Chem. Eng. 9, 106286 https://doi.org/10.1016/j.jece.2021.106286.

Koskue, V., Rinta-kanto, J.M., Freguia, S., Ledezma, P., Kokko, M., 2021b. Optimising nitrogen recovery from reject water in a 3-chamber bioelectroconcentration cell. Separ. Purif. Technol. 264, 118428 https://doi.org/10.1016/j.seppur.2021.118428.

Kwan, T.H., Hu, Y., Lin, C.S.K., 2018. Techno-economic analysis of a food waste valorisation process for lactic acid, lactide and poly(lactic acid) production. J. Clean. Prod. 181, 72–87. https://doi.org/10.1016/j.jclepro.2018.01.179.

Lackner, S., Gilbert, E.M., Vlaeminck, S.E., Joss, A., Horn, H., van Loosdrecht, M.C.M., 2014. Full-scale partial nitritation/anammox experiences - an application survey. Water Res. 55, 292–303. https://doi.org/10.1016/j.watres.2014.02.032.

Metcalf, Eddy, I., 2014. Wastewater Engineering. Treatment and Resource Recovery, fifth ed. McGraw-Hill Education.

Methanex, 2022. Methanex Methanol Price Sheet. Regional Posted Contract Prices.

Nancharaiah, Y.V., Venkata Mohan, S., Lens, P.N.L., 2016. Recent advances in nutrient removal and recovery in biological and bioelectrochemical systems. Bioresour. Technol. 215, 173–185. https://doi.org/10.1016/j.biortech.2016.03.129.

Rockström, J., Steffen, W., Noone, K., Persson, Å., Chapin, F.S.I., Lambin, E.F., Lenton, T.M., Scheffer, M., Folke, C., Schellnhuber, H.J., Nykvist, B., de Wit, C.A., Hughes, T., van der Leeuw, S., Rodhe, H., Sörlin, S., Snyder, P.K., Costanza, R., Svedin, U., Falkenmark, M., Karlberg, L., Corell, R.W., Fabry, V.J., Hansen, J., Walker, B., Liverman, D., Richardson, K., Crutzen, P., Foley, J.A., 2009. A safe operating space for humanity. Nature 461, 472–475.

Rodrigues, M., De Mattos, T.T., Sleutels, T., Ter Heijne, A., Hamelers, H.V.M., Buisman, C.J.N., Kuntke, P., 2020. Minimal bipolar membrane cell configuration for scaling up ammonium recovery. ACS Sustain. Chem. Eng. 8, 17359–17367. https://doi.org/10.1021/acssuschemeng.0c05043.

Rodríguez Arredondo, M., Kuntke, P., ter Heijne, A., Hamelers, H.V.M., Buisman, C.J.N., 2017. Load ratio determines the ammonia recovery and energy input of an electrochemical system. Water Res. 111, 330–337. https://doi.org/10.1016/j.watres.2016.12.051.

Rozendal, R.A., Hamelers, H.V.M., Rabaey, K., Keller, J., Buisman, C.J.N., 2008. Towards practical implementation of bioelectrochemical wastewater treatment. Trends Biotechnol. 26, 450–459. https://doi.org/10.1016/j.tibtech.2008.04.008.

Solon, K., Volcke, E.I.P., Spérandio, M., van Loosdrecht, M.C.M., 2019. Resource recovery and wastewater treatment modelling. Environ. Sci. Water Res. Technol. 631–642. https://doi.org/10.1039/c8ew00765a.

Sutton, M., Bleeker, A., Howard, C., Bekunda, M., Grizzetti, B., de Vries, W., van Grinsven, H., Abrol, Y., Adhya, T., Billen, G., Davidson, E., Datta, A., Diaz, R., Erisman, J., Liu, X., Oenema, O., Palm, C., Raghuram, N., Reis, S., Scholz, R., Sims, T., Westhoek, H., Fs, Z., 2013. Our nutrient world: the challenge to produce more food and energy with less pollution. Global overview of nutrient management.

Vaneeckhaute, C., Claeys, F.H.A., Tack, F.M.G., Meers, E., Belia, E., Vanrolleghem, P.A., 2018. Development, implementation, and validation of a generic nutrient recovery model (NRM) library. Environ. Model. Software 99, 170–209. https://doi.org/10.1016/j.envsoft.2017.09.002.

Vaneeckhaute, C., Lebuf, V., Michels, E., Belia, E., Vanrolleghem, P.A., Tack, F.M.G., Meers, E., 2017. Nutrient recovery from digestate: systematic technology review and product classification. Waste and Biomass Valorization 8, 21–40. https://doi.org/10.1007/s12649-016-9642-x.

Volcke, E.I.P., Gernaey, K.V., Vrecko, D., Jeppsson, U., Van Loosdrecht, M.C.M., Vanrolleghem, P.A., 2006. Plant-wide (BSM2) evaluation of reject water treatment with a SHARON-anammox process. Water Sci. Technol. 54, 93–100. https://doi.org/10.2166/wst.2006.822.

Wang, M., Khan, M.A., Mohsin, I., Wicks, J., Ip, A.H., Sumon, K.Z., Dinh, C.-T., Sargent, E.H., Gates, I.D., Kibria, M.G., 2021. Can sustainable ammonia synthesis pathways compete with fossil-fuel based Haber–Bosch processes? Energy Environ. Sci. 2535–2548. https://doi.org/10.1039/d0ee03808c.

Ward, A.J., Arola, K., Thompson Brewster, E., Mehta, C.M., Batstone, D.J., 2018. Nutrient recovery from wastewater through pilot scale electrodialysis. Water Res. 135, 57–65. https://doi.org/10.1016/j.watres.2018.02.021.

Wu, X., Modin, O., 2013. Ammonium recovery from reject water combined with hydrogen production in a bioelectrochemical reactor. Bioresour. Technol. 146, 530–536. https://doi.org/10.1016/j.biortech.2013.07.130.